Geophysical Research Letters

RESEARCH LETTER
10.1029/2025GL117527

Role of Active Folding in Rupture Arrest of a Great Thrust Earthquake

Weiwang Long[1], Zhigang Li[1,2], Yanjun Wang[3,4], Rafael Almeida[5], Giovanni Camanni[6], Chuang Sun[7], Weitao Wang[1,2], Chuanyong Wu[8], Xiangming Dai[1], Wen Sun[1], Xiancan Wu[1], Lianwen Wu[1], Jie Lin[1], and Peizhen Zhang[1,2]

[1]Guangdong Provincial Key Lab of Geodynamics and Geohazards, School of Earth Sciences and Engineering, Sun Yat-sen University, Zhuhai, China, [2]Southern Marine Science and Engineering Guangdong Laboratory (Zhuhai), Zhuhai, China, [3]Key Laboratory of Reservoir Characterization, China National Petroleum Corporation, Lanzhou, China, [4]Research Institute of Petroleum Exploration & Development-Northwest, PetroChina, Lanzhou, China, [5]Department of Geological Sciences, San Diego State University, San Diego, CA, USA, [6]Dipartimento di Scienze Chimiche e Geologiche, Università di Modena e Reggio Emilia, Modena, Italy, [7]College of Earth Sciences, Jilin University, Changchun, China, [8]Institute of Disaster Prevention, Sanhe, China

Abstract Understanding the cause and location of the end-points of thrust earthquake ruptures is critical yet unresolved question in seismic hazard assessment for convergent margins, where numerous destructive earthquakes have occurred. Here, we offer a novel perspective on rupture termination by examining the arrest of the 1906 M 8.0 Manas earthquake in northwestern China. Integrated field surveys, seismic profiles, and microseismicity data reveal that rupture terminated at the actively growing Xiaodushan anticline. This anticline lies parallel to and in the hanging wall of the seismogenic fault. We propose active folding acts as an efficient rupture-arrest barrier, partitioning seismic energy into strata uplift and microseismicity. Furthermore, comparative analysis of global thrust earthquakes identifies two termination mechanisms: fault geometric complexities and external structural barriers. These findings contribute to deeper understanding of rupture lengths and earthquake magnitudes for seismic hazard assessment in convergent margins globally.

Plain Language Summary "Why and where do thrust earthquakes stop?" remains a key question in assessing seismic hazards along convergent plate boundaries. This study examines the 1906 M 8.0 Manas earthquake in northwestern China and proposes a new mechanism for rupture termination. Through field survey of surface ruptures, 3D modeling of the seismogenic fault, and comparative analysis of structural deformation, we find that the rupture likely halted at an actively growing fold. We suggest that such active folding can act as a physical barrier, diverting seismic energy into crustal uplift and distributed microseismicity, thereby preventing further rupture propagation. A global comparison of similar events reveals two primary termination processes: either rupture is disrupted by complex fault geometries, or energy is absorbed by external structures such as active folds. These findings help us better understand how far earthquakes can spread and how strong they can get, which is important for assessing earthquake risks in convergent margins.

Key Points:

- Active folds act as effective rupture-arrest barriers by dissipating seismic energy via crustal uplift and microseismicity
- Rupture termination in global thrust earthquakes occurs through two primary mechanisms: internal fault geometric complexities and external structural barriers
- These findings enhance seismic hazard assessment by clarifying the key factors controlling rupture arrest in global convergent margins

Supporting Information:

Supporting Information may be found in the online version of this article.

Correspondence to:

Z. Li and Y. Wang,
lizhigang@mail.sysu.edu.cn;
wang_yj8@petrochina.com.cn

Citation:

Long, W., Li, Z., Wang, Y., Almeida, R., Camanni, G., Sun, C., et al. (2025). Role of active folding in rupture arrest of a great thrust earthquake. *Geophysical Research Letters*, *52*, e2025GL117527. https://doi.org/10.1029/2025GL117527

Received 12 JUN 2025
Accepted 6 SEP 2025

Author Contributions:

Conceptualization: Weiwang Long, Zhigang Li, Peizhen Zhang
Data curation: Yanjun Wang, Chuanyong Wu
Formal analysis: Weiwang Long, Zhigang Li, Yanjun Wang, Rafael Almeida, Giovanni Camanni, Chuang Sun, Weitao Wang, Lianwen Wu, Jie Lin, Peizhen Zhang
Funding acquisition: Zhigang Li, Peizhen Zhang
Investigation: Weiwang Long, Zhigang Li, Weitao Wang,

1. Introduction

One of the central issues of earthquake hazard assessment is how to estimate rupture lengths and magnitudes of potential earthquakes along seismogenic faults (Leonard, 2010; Scholz, 1982). Understanding factors that affect the arrest of a rupture is crucial for seismic hazard analysis, as longer ruptures generally result in larger earthquakes (C. M. Rubin, 1996). Since the introduction of concepts like barriers and asperities (Aki, 1979; King & Nábělek, 1985), extensive research on strike slip faults have demonstrated that geometric complexities (e.g., fault bends, branches, and stepovers) can control the initiation, propagation, and termination of earthquake ruptures, thereby determining earthquake magnitudes (Biasi & Wesnousky, 2016; Wesnousky, 2006).

Similar studies on thrust earthquakes have focused on coseismic slip variations caused by fault geometric complexities (Hubbard et al., 2016; T. Li et al., 2019; Williams et al., 2024). Great thrust earthquakes, however, exhibit complex and irregular rupture patterns and are generally less likely to be terminated by fault steps or branches than strike-slip earthquakes (Biasi & Wesnousky, 2016). Relying solely on fault geometric segmentation may result in an oversimplified assessment of seismic behavior (C. M. Rubin, 1996). Consequently, the

Xiangming Dai, Wen Sun, Xiancan Wu, Peizhen Zhang
Methodology: Weiwang Long, Xiangming Dai, Wen Sun, Xiancan Wu
Resources: Zhigang Li, Peizhen Zhang

study of rupture termination patterns and mechanisms in thrust earthquakes remains unresolved, which hinders the accuracy of seismic hazard assessments in convergent tectonic settings.

This study examines the surface rupture characteristics of the 1906 M 8.0 Manas earthquake within the active Northern Tian Shan fold-thrust belt. The earthquake is interpreted to have initiated at ∼20 km depth along Southern Junggar thrust (SJT) and produced a surface rupture extending approximately 130 km (Avouac et al., 1993; Deng et al., 1996; Stockmeyer et al., 2014), breaching several large geometric segment boundaries along the Huoerguosi-Manas-Tugulu fold system (Figure 1a). Notably, its surface rupture termination is located in a region lacking significant variations in fault geometry, lithology, or geomorphology (Figure 1 and Figure S1 in Supporting Information S1), which leaves the causal mechanisms underlying the rupture arrest unclear.

Here, we integrate 2D seismic reflection profiles, surface topography, microseismicity data ($M_L > 2$), and a 3D model of the SJT to investigate the factors that led to rupture termination of the Manas earthquake. We then systematically analyze the barriers that influence the propagation of thrust earthquakes, thereby providing valuable insights for seismic hazard assessment in convergent tectonic settings.

2. Geological Setting

As one of the most significant and largest mountain ranges in Central Asia, the Tian Shan mountain belt has undergone a complex tectonic evolution, with pre-Cenozoic structures reactivated due to the collision of the Asia-Europe plates (Avouac et al., 1993; Deng et al., 2000). This tectonic activity significantly reshaped the landscape, giving rise to distinct structures such as the fold-thrust belt on the northern margin of the Tian Shan Mountains (C. Li et al., 2011; H. Lu et al., 2019), which forms a series of east-west trending *en échelon* anticlines in the Junggar Basin (Figure 1, Deng et al., 2000). This fold-thrust belt comprises four asymmetric anticlines, including the Huoerguosi, Manas, Tugulu, and Xiaodushan folds. These structures are interpreted to connect to a deep ramp of the SJT through a Paleogene décollement (Figure S12 in Supporting Information S1). The deep ramp extends much farther laterally than the upper fault ramp. Magnetostratigraphic analysis of growth strata reveals that these anticlines began forming around ∼6–10 Ma (H. Lu et al., 2019).

As the dominant seismogenic structure in the Northern Tian Shan orogenic belt, the SJT has generated multiple historical earthquakes, including the 1906 M 8.0 Manas and the 2016 M_W 6.2 Hutubi earthquake. The former event exhibited a broader rupture zone and deeper hypocenter compared to the latter, which primarily ruptured a secondary fault along the SJT (R. Lu et al., 2018). In this work, we conducted a detail investigation of the eastern termination of the Manas earthquake adjacent to the Xiaodushan anticline (Figure 1 and Figure S1 in Supporting Information S1).

3. Data and Methods

3.1. Field Observation and Topographic Surveying

To validate subsurface structural interpretations and characterize surface morphology of the Manas earthquake rupture area, comprehensive field investigations were conducted in the region of the Xiaodushan anticline (Figure 2a). We then constructed a geological cross-section parallel to the Hutubi River and measured bedding attitudes west of this section to delimit the Tugulu and Xiaodushan anticlines (Figure 2a and Figure S2 in Supporting Information S1). Finally, A 12.5 m resolution DEM was processed in ArcGIS to generate strike-parallel swath profile across the fold crest (Figure 2a and Figure S3 in Supporting Information S1).

3.2. Seismic Data and Structure Interpretation

Seven seismic reflection profiles (lines AA'-GG') oriented perpendicular to regional structural strike were analyzed to quantify subsurface structural geometries and shortening variations (Figure 2b and Figures S6–S11 in Supporting Information S1). Regional average velocity model (3,000 m/s) was applied for depth conversion, and stratigraphy was interpreted in the profiles using drill hole data (Qiu et al., 2019). We employed area-depth-strain (ADS) analysis and balanced cross-section methods to calculate the shortening for these profiles (see Text S3 in Supporting Information S1). ADS analysis uses variations in fold area with depth to quantify structural shortening (Rivas-Dorado, 2023). We interpreted 17 seismic profiles spanning the strike of the Huoerguosi-Manas-Tugulu structural belt (Figure 1) and reconstructed a 3D fault model in SKUA-GOCAD software to investigate the seismogenic structures and subsurface geometry of the earthquake area (Figure 3). Microseismic records since

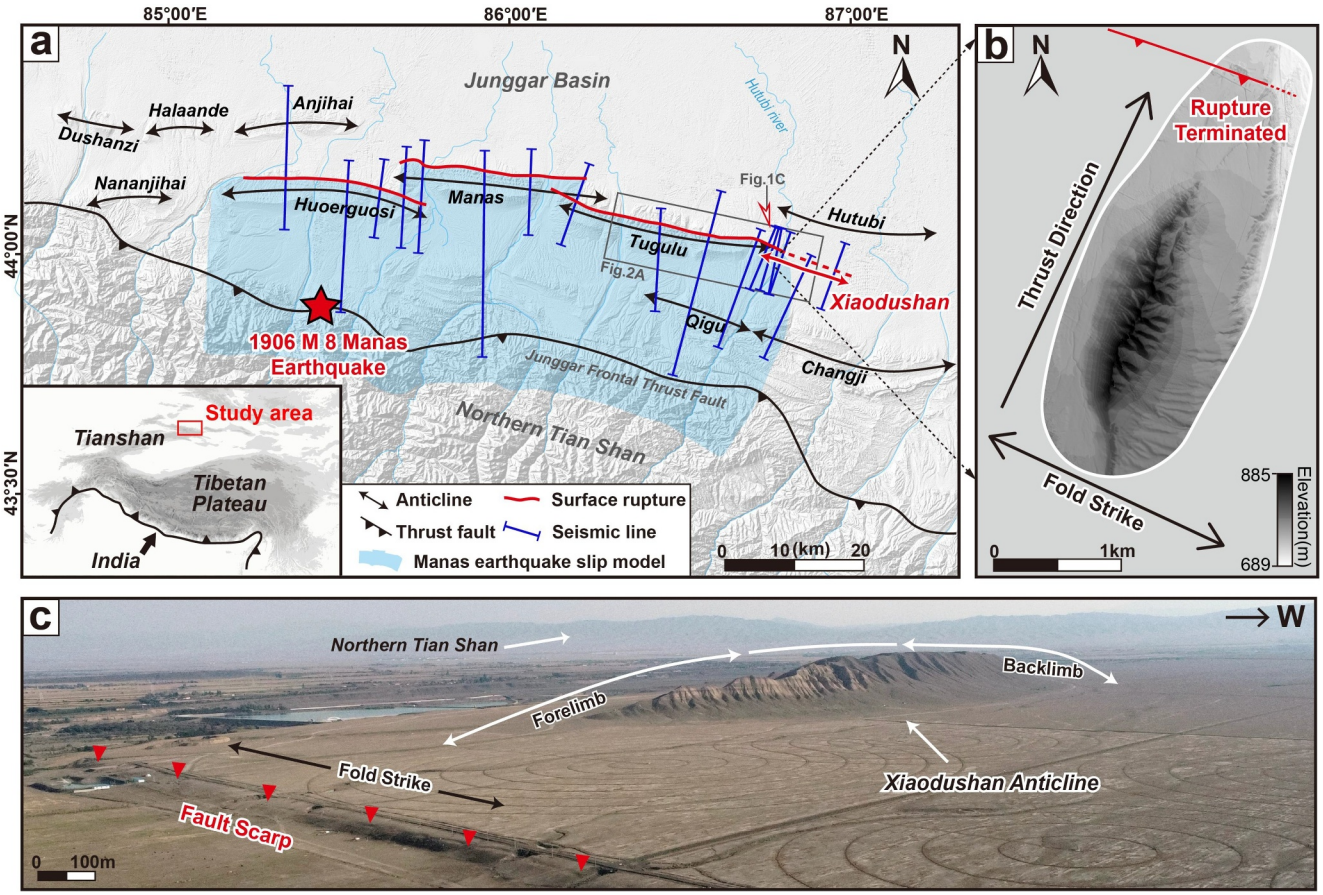

Figure 1. General overview map of the study area. (a) Simplified geological map of the Northern Tian Shan fold-thrust belt, the inset map indicates the location of the study area. (b) Structural characteristics of the Xiaodushan anticline, high-resolution DEM was generated by unmanned aerial vehicle. (c) General view of the Xiaodushan anticline and fault scarp of 1906 M 8.0 Manas earthquake.

1970 have been utilized to analyze the spatial distribution of micro-earthquake hypocenters following Manas and Hutubi events (Figure 3a, Figures S4 and S5 in Supporting Information S1).

4. Results

Our field survey revealed that the Xiaodushan anticline predominantly exposes the N_2d and the Q_1x Formation, with gently inclined strata (0°–20°) in the southern backlimb and steeper strata (50°–60°) in the northern forelimb (Figure 2b and Figure S2 in Supporting Information S1). Furthermore, we observed a continuous sequence of growth strata (~220 m) within the backlimb of the Xiaodushan anticline (Figure S2 in Supporting Information S1). Combining the measured growth-strata thickness with Quaternary sediment accumulation rates estimated at the Tugulu anticline (~260 m/Ma, Figure 2a; C. Li et al., 2011) allow us to estimate that the Xiaodushan anticline formed at ~0.8 Ma.

A swath profile along the crest of the of the Tugulu anticline (pink line in Figure 2c) forms an upwardly convex shape from its core to its tip. We note that the strata at the eastern tip of the Tugulu anticline dip eastward, and those at the western limb of the Xiaodushan anticline dip westward (Figure 2a and Figure S1c in Supporting Information S1). Surface expression of the Xiaodushan anticline has been almost completely removed by erosion of Hutubi River (Figure 1c).

The shortening distribution along the Tugulu and Xiaodushan anticlines exhibits a spatial pattern similar to that of topographic changes (Figure 2c). An abrupt decrease to minima occurs precisely at the structural transition zone between the Tugulu and Xiaodushan anticlines, as evidenced by the sharp displacement variations marked by the blue line in Figure 2c.

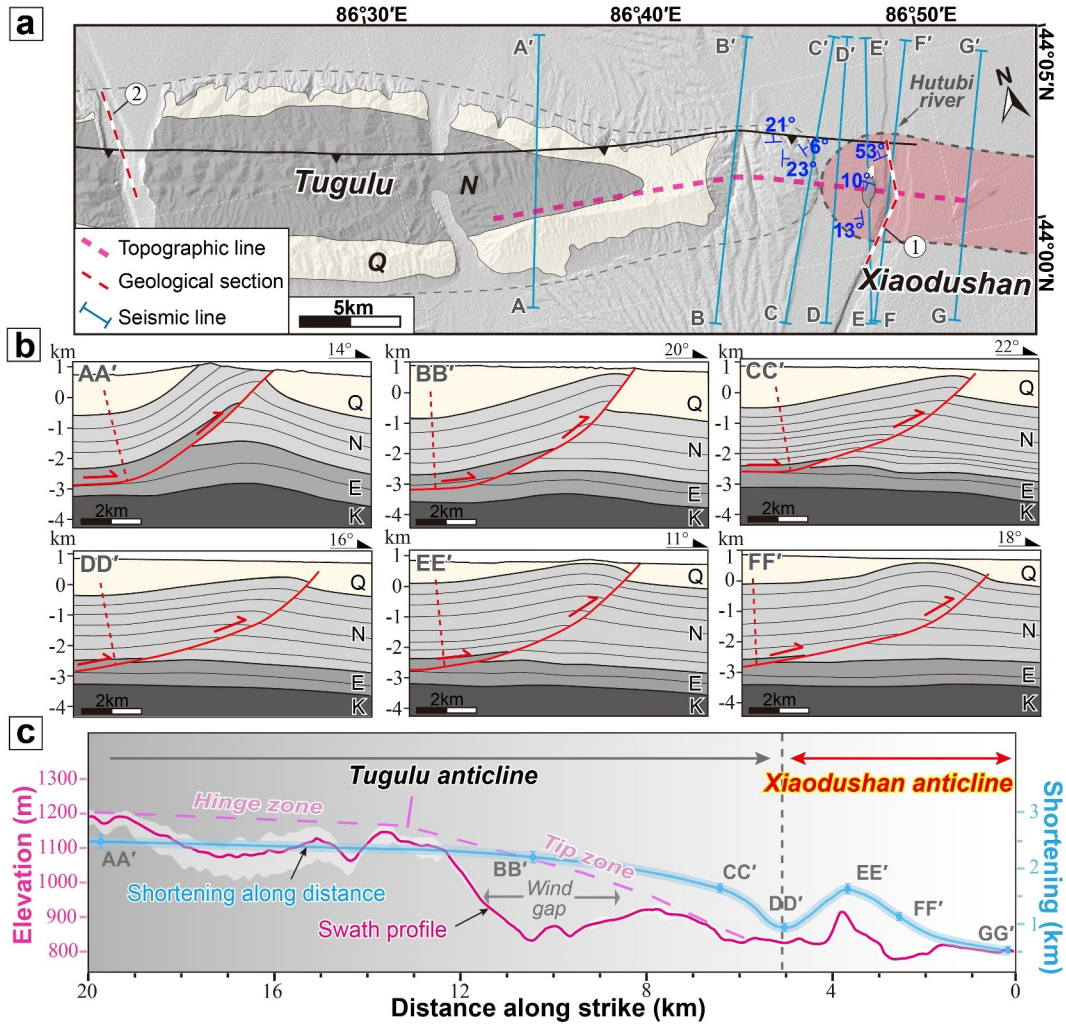

Figure 2. (a) Simple geological map of the Xiaodushan anticline and adjacent regions. Dashed pink line shows the location of the swath profile in panel (c). The red dash lines show the locations of the geological section (② from C. Li et al. (2011)). (b) Interpreted seismic reflection profiles across the Xiaodushan anticline and Tugulu anticline; Abbreviations: Q-Quaternary, N-Neogene, E-Eocene, and K-Cretaceous. (c) Diagram showing along-fold profiles of topography (pink line) and shortening (thick blue line) measured in cross sections constructed from seismic reflection lines (e.g., panel (b)).

The 3D fault model shows that the Huoerguosi-Manas-Tugulu ramp segments are offset by 9 and 5 km, respectively, but are connected to the deep-seated SJT through a décollement at a depth of approximately 4–5 km (Figure 3a). There is little geometric complexity along strike on the lower ramp of the SJT, except that the décollement above the ramp gradually widens eastward (Figure 3a). Microseismic data indicate two distinct clusters elongated along the longitudinal direction (Figure 3a). One at the site of the 2016 Hutubi M_W 6.0 earthquake (R. Lu et al., 2018) and another at the Xiaodushan anticline. Focal depth analysis of both clusters shows that the Xiaodushan region exhibits broader depth distribution and greater concentration of microseismic events (Text S4 and Figure S5 in Supporting Information S1).

5. Discussion

5.1. Active Folding Arrests Great Thrust Earthquake Ruptures

Compared with surrounding structures, the Xiaodushan anticline shows lower deformation magnitude (Figure 2c), younger formation age, and an immature underlying fault (Figure 3b). These features indicate that it is not the tip of the Tugulu anticline, as previously proposed, but rather an independently growing fold.

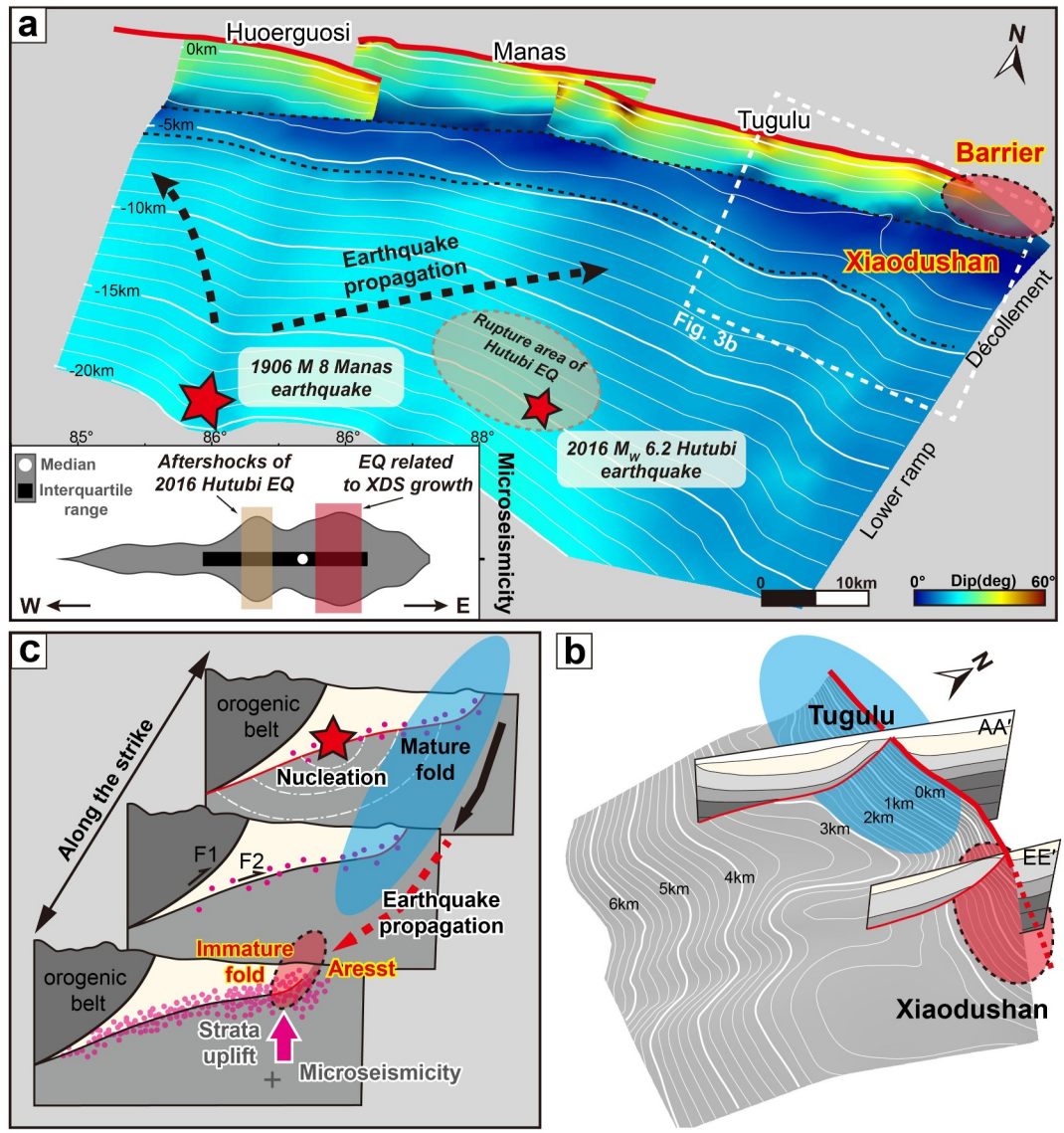

Figure 3. (a) 3D fault model for 1906 Manas earthquake and spatial density map of microseismic activity along fault strike. The red solid line represents the exposed surface trace of the Manas earthquake. The thin dashed black lines represent the décollement surface. (b) Subsurface 3D structure of the Xiaodushan anticline. (c) A schematic diagram illustrating the mechanism of active folds stopping thrust earthquake propagation.

Paleoseismic trenching and fault scarp analyses (Figure S3 in Supporting Information S1, Avouac et al., 1993; Deng et al., 1996) constrained the 1906 Manas rupture to the central SJT fault, terminating abruptly east of the Hutubi River without reaching the Changji and Hutubi anticlines (Figure S3b in Supporting Information S1). Our 3D kinematic model reveals only minor along-strike dip variation across this segment (Figure 3a), ruling out fault geometry as the primary control. Instead, seismic profiles and deformation analyses indicate that rupture stopped precisely where the Xiaodushan anticline is actively developing (Figure 2 and Figure S3 in Supporting Information S1).

Seismicity further supports this interpretation (Figure 3a and Figure S4 in Supporting Information S1). Our analysis reveals a systematic eastward increase in microseismic event density along the fold belt. In contrast, seismicity in the main rupture zone of the Huo-Ma-Tu fault belt is sparse (Figure S4 in Supporting Information S1). The seismicity cluster beneath Xiaodushan may reflect background seismicity related to ongoing fold growth (Figure 3c). Recent studies show that the fold uplift can be partly seismic, as flexural bending and fracture

propagation in layered strata induce bedding-parallel slip (Gràcia et al., 2019; Huang et al., 2024). At the early stages of fold growth, rapid strata uplift and fault slip gradually release tectonic loading energy, altering the regional stress state (Nabavi & Fossen, 2021). This process resembles the locked-creeping segmentation observed in strike-slip faults, where some sections slip aseismically while others remain locked (Chen & Bürgmann, 2017; Harris, 2017). During seismic cycles, mature faults like Huo-Ma-Tu thrust are prone to release accumulated elastic strain catastrophically, whereas the Xiaodushan segment—with ongoing microseismicity (Figure S4 in Supporting Information S1) and progressive growth (Figure S2e in Supporting Information S1)—likely accommodates deformation largely aseismically, reducing its coseismic slip potential and acting as an effective rupture barrier (Figure 3c).

An alternative explanation is that rupture slip transferred into distributed folding at the termination area, and the observed seismicity represents prolonged aftershocks of the 1906 event. Although century-long aftershock sequences are uncommon, they have been reported in many historical cases (e.g., Stein & Liu, 2009; Toda & Stein, 2018). In this scenario, coseismic energy release at the rupture terminus may have modified local stresses, sustaining long-lived afterslip (Diao et al., 2021; A. M. Rubin et al., 1999).

On longer timescales, rupture arrest and fold growth may reinforce each another: arrested ruptures promote strata folding, while fold growth enhances the barrier effect. However, prolonged aftershock activity is more typical of intraplate settings than of the high-strain-rate orogen like Tian Shan (Stein & Liu, 2009). From this perspective, we favor that active fold growth functions as energy incompatibilities that substantially arrests earthquake rupture propagation (Figure 3c).

5.2. Comparison to Other Thrust Earthquake Rupture Terminations

The contrasting mechanical behaviors of thrust and strike-slip systems yield fundamentally different rupture propagation responses to structural barriers. Thrust faults can propagate across larger steps compared to strike-slip faults (Biasi & Wesnousky, 2016). In this study, the 1906 Manas earthquake even ruptured through a fault step exceeding 9 km in the Huo-Ma-Tu structural belt (Figure 3a). Earthquakes rooted in deep décollements can activate all overlying branch faults, whereas those along branch faults may arrest rupture (T. Li et al., 2019). Additionally, sharper fault bends increase the likelihood of rupture arrest due to enhanced stress concentration, particularly in regions with pronounced curvature (Biasi & Wesnousky, 2021; Figure 4a). These findings emphasize the importance of integrating source depth and fault curvature metrics in geometric barrier analyses.

Our study reveals that the termination of thrust earthquake rupture requires consideration of both fault geometric complexities and external structural barriers along propagation paths (Figure 4). Analysis of numerous large thrust earthquakes reveal that their rupture propagation is commonly inhibited by pre-existing faults, folds, or crystalline massif (Figures 4c–4e). On large subduction interfaces, analogous features such as seamounts, fracture zones, and plate boundaries can facilitate termination of seismic rupture propagation (Figure 4f). These geological discontinuities may induce local stress state perturbations, thereby affecting the propagation behavior of seismic ruptures.

While this study provides a foundational framework, two inherent limitations should be acknowledged. First, the absence of high-resolution geodetic observations such as InSAR or continuous GPS limits our ability to directly monitor deformation associated with fold growth. Second, we did not conduct dynamic rupture simulations capable of reproducing the transient processes that arrest rupture propagation at structural barriers. Integrating our observations with high-resolution geodetic monitoring, laboratory friction experiments, and numerical modeling (Biasi & Wesnousky, 2021; Ke et al., 2018) will advance mechanistic understanding of rupture termination processes and improve predictive capabilities for convergent margin settings.

6. Conclusions

Integrated topographic, tectonic, and geochronologic analyses reveal active growth of the Xiaodushan anticline. Field documentation of the 1906 Manas M 8.0 earthquake termination zone, combined with 3D fault modeling, demonstrates spatial correlation between rupture arrest, fold growth, and microseismicity. We propose that active folds impede thrust rupture propagation by dissipating seismic energy through strata uplift and microseismicity. Analysis of global fold-thrust belt earthquakes establishes two rupture termination mechanisms: (a) seismogenic

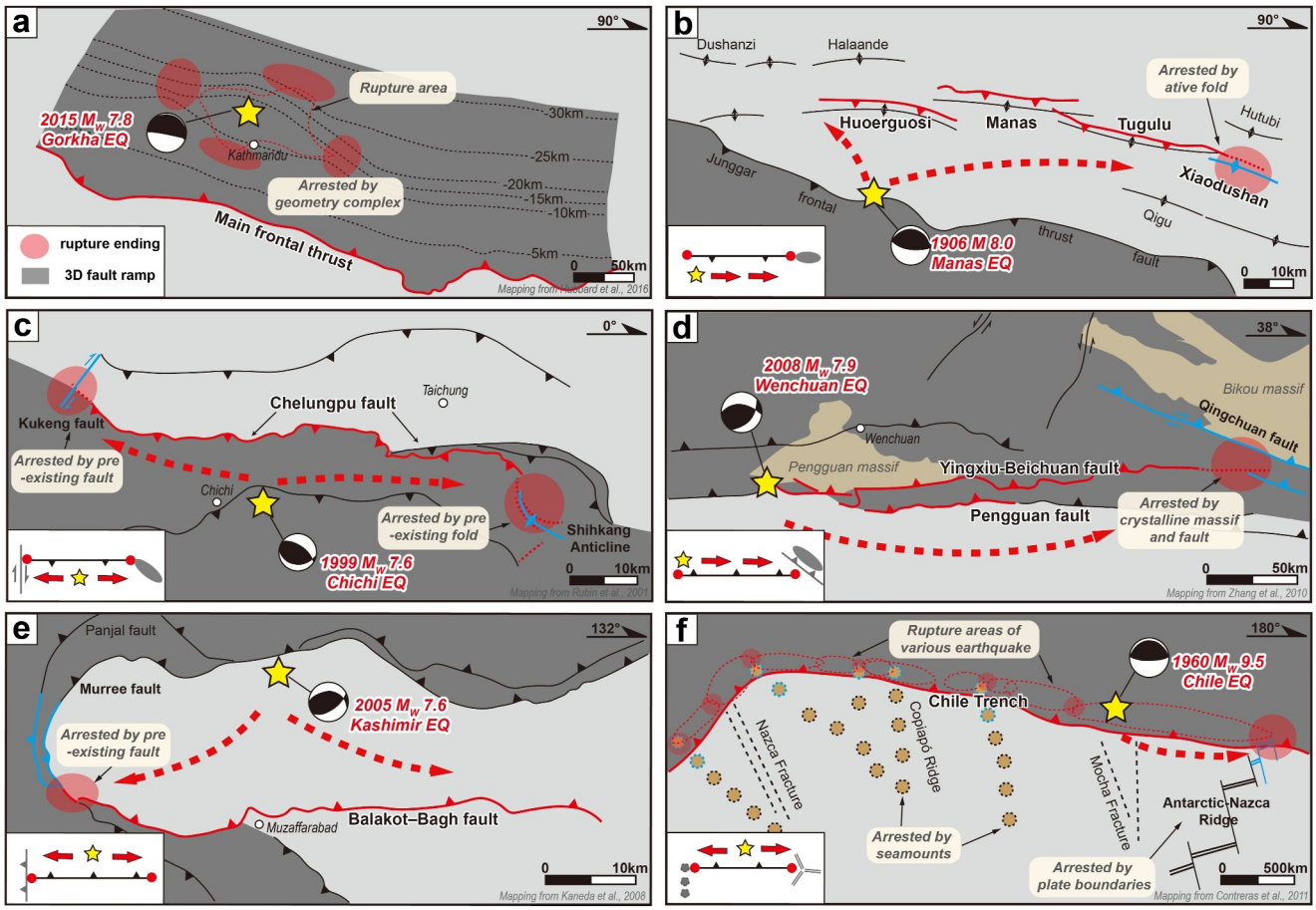

Figure 4. Examples demonstrate the rupture zones of classical thrust earthquakes and the analysis of their termination barriers. The dark and light gray represent the foothills and plains, respectively. The blue line marks the barriers, while the red shading indicates the termination zones. (a) 2015 MW 7.8 Gorkha (Hubbard et al., 2016). (b) 1906 M 8 Manas. (c) 1999 MW 7.6 Chichi (C. M. Rubin et al., 2001). (d) 2008 MW 8.0 Wenchuan (Zhang et al., 2010). (e) 2005 MW 7.6 Kashimir (Kaneda et al., 2008). (f) 1960 MW 9.5 Chile (Contreras-Reyes & Carrizo, 2011).

fault geometric complexities and (b) external structural barriers. These findings advance understanding of thrust earthquake rupture arrest and enhance seismic hazard assessment.

Conflict of Interest

The authors declare no conflicts of interest relevant to this study.

Data Availability Statement

The 30 m-resolution digital elevation model used in Figure 1a are obtained from https://www.gscloud.cn. The 12.5 m-resolution digital elevation model data used in Figure 2a are obtained from https://search.asf.alaska.edu. The seismic data and microseismic records since 1970 are uploaded to Zenodo and available at https://doi.org/10.5281/zenodo.16925273 (Long, 2025). The SKUA-GoCAD software used for constructing 3D structural model is provided by Institute of Geology, China Earthquake Administration.

Acknowledgments
We acknowledge the constructive comments provided by Editor Daoyuan Sun, Associate Editor Ake Fagereng, and reviewers Andy Nicol and anonymous reviewer during the rivision of our manuscript. We are also grateful to Professor Xuhua Shi, Gang Rao, Qiang Qiu and Qin Jintang for their valuable discussions. This research was jointly supported by the National Natural Science Foundation of China (42030301 and 42172233) and the National Key Research and Development Project of China (Grant 2023YFC3008600).

References

Aki, K. (1979). Characterization of barriers on an earthquake fault. *Journal of Geophysical Research*, *84*(B11), 6140–6148. https://doi.org/10.1029/JB084iB11p06140

Avouac, J. P., Tapponnier, P., Bai, M., You, H., & Wang, G. (1993). Active thrusting and folding along the northern Tien Shan and late Cenozoic rotation of the Tarim relative to Dzungaria and Kazakhstan. *Journal of Geophysical Research*, *98*(B4), 6755–6804. https://doi.org/10.1029/92JB01963

Biasi, G. P., & Wesnousky, S. G. (2016). Steps and gaps in ground ruptures: Empirical bounds on rupture propagation. *Bulletin of the Seismological Society of America*, *106*(3), 1110–1124. https://doi.org/10.1785/0120150175

Biasi, G. P., & Wesnousky, S. G. (2021). Rupture passing probabilities at fault bends and steps, with application to rupture length probabilities for earthquake early warning. *Bulletin of the Seismological Society of America*, *111*(4), 2235–2247. https://doi.org/10.1785/0120200370

Chen, K. H., & Bürgmann, R. (2017). Creeping faults: Good news, bad news? *Reviews of Geophysics*, *55*(2), 282–286. https://doi.org/10.1002/2017RG000565

Contreras-Reyes, E., & Carrizo, D. (2011). Control of high oceanic features and subduction channel on earthquake ruptures along the Chile–Peru subduction zone. *Physics of the Earth and Planetary Interiors*, *186*(1–2), 49–58. https://doi.org/10.1016/j.pepi.2011.03.002

Deng, Q., Feng, X., Zhang, P., Xu, X., Yang, X., Peng, S., & Li, J. (2000). *Active tectonics of the Tian Shan Mountains (in Chinese)*. Seismology Press.

Deng, Q., Zhang, P., Xu, X., Yang, X., Peng, S., & Feng, X. (1996). Paleoseismology of the northern piedmont of Tianshan Mountains, northwestern China. *Journal of Geophysical Research*, *101*(B3), 5895–5920. https://doi.org/10.1029/95JB02739

Diao, F., Wang, R., Xiong, X., & Liu, C. (2021). Overlapped postseismic deformation caused by afterslip and viscoelastic relaxation following the 2015 Mw 7.8 Gorkha (Nepal) earthquake. *Journal of Geophysical Research: Solid Earth*, *126*(3), e2020JB020378. https://doi.org/10.1029/2020JB020378

Gràcia, E., Grevemeyer, I., Bartolomé, R., Perea, H., Martínez-Loriente, S., Gómez De La Peña, L., et al. (2019). Earthquake crisis unveils the growth of an incipient continental fault system. *Nature Communications*, *10*(1), 3482. https://doi.org/10.1038/s41467-019-11064-5

Harris, R. A. (2017). Large earthquakes and creeping faults. *Reviews of Geophysics*, *55*(1), 169–198. https://doi.org/10.1002/2016RG000539

Huang, K., Chen, K., Wu, L., Shi, X., Wei, G., Zhang, J., et al. (2024). Buckling contributes to both coseismic uplift and long-term fold growth in active fold-thrust belts. *Geology*, *53*(1), 61–66. https://doi.org/10.1130/G52422.1

Hubbard, J., Almeida, R., Foster, A., Sapkota, S. N., Bürgi, P., & Tapponnier, P. (2016). Structural segmentation controlled the 2015 Mw 7.8 Gorkha earthquake rupture in Nepal. *Geology*, *44*(8), 639–642. https://doi.org/10.1130/G38077.1

Kaneda, H., Nakata, T., Tsutsumi, H., Kondo, H., Sugito, N., Awata, Y., et al. (2008). Surface rupture of the 2005 Kashmir, Pakistan, earthquake and its active tectonic implications. *Bulletin of the Seismological Society of America*, *98*(2), 521–557. https://doi.org/10.1785/0120070073

Ke, C., McLaskey, G. C., & Kammer, D. S. (2018). Rupture termination in laboratory-generated earthquakes. *Geophysical Research Letters*, *45*(23), 12784–12792. https://doi.org/10.1029/2018GL080492

King, G., & Nábělek, J. (1985). Role of fault bends in the initiation and termination of earthquake rupture. *Science*, *228*(4702), 984–987. https://doi.org/10.1126/science.228.4702.984

Leonard, M. (2010). Earthquake fault scaling: Self-consistent relating of rupture length, width, average displacement, and moment release. *Bulletin of the Seismological Society of America*, *100*(5A), 1971–1988. https://doi.org/10.1785/0120090189

Li, C., Dupont-Nivet, G., & Guo, Z. (2011). Magnetostratigraphy of the northern Tian Shan foreland, taxi He section, China: Magnetostratigraphy of the northern Tian Shan foreland. *Basin Research*, *23*(1), 101–117. https://doi.org/10.1111/j.1365-2117.2010.00475.x

Li, T., Chen, Z., Chen, J., Thompson Jobe, J. A., Burbank, D. W., Li, Z., et al. (2019). Along-strike and downdip segmentation of the Pamir frontal thrust and its association with the 1985 *Mw* 6.9 Wuqia earthquake. *Journal of Geophysical Research: Solid Earth*, *124*(9), 9890–9919. https://doi.org/10.1029/2019JB017319

Long, W. (2025). Role of active folding in rupture arrest of a great thrust earthquake [Dataset]. *Zenodo*. https://doi.org/10.5281/zenodo.16925273

Lu, H., Li, B., Wu, D., Zhao, J., Zheng, X., Xiong, J., & Li, Y. (2019). Spatiotemporal patterns of the late Quaternary deformation across the northern Chinese Tian Shan foreland. *Earth-Science Reviews*, *194*, 19–37. https://doi.org/10.1016/j.earscirev.2019.04.026

Lu, R., He, D., Xu, X., Wang, X., Tan, X., & Wu, X. (2018). Seismotectonics of the 2016 M 6.2 Hutubi earthquake: Implications for the 1906 M 7.7 Manas earthquake in the Northern Tian Shan Belt, China. *Seismological Research Letters*, *89*(1), 13–21. https://doi.org/10.1785/0220170123

Nabavi, S. T., & Fossen, H. (2021). Fold geometry and folding – A review. *Earth-Science Reviews*, *222*, 103812. https://doi.org/10.1016/j.earscirev.2021.103812

Qiu, J., Rao, G., Wang, X., Yang, D., & Xiao, L. (2019). Effects of fault slip distribution on the geometry and kinematics of the southern Junggar fold-and-thrust belt, northern Tian Shan. *Tectonophysics*, *772*, 228209. https://doi.org/10.1016/j.tecto.2019.228209

Rivas-Dorado, S. (2023). Estimation of detachment depths and displacements from the area–depth markers of contractional growth structures: Testing the "inverse line" concept. *AAPG Bulletin*, *107*(3), 413–443. https://doi.org/10.1306/09232220096

Rubin, A. M., Gillard, D., & Got, J.-L. (1999). Streaks of microearthquakes along creeping faults. *Nature*, *400*(6745), 635–641. https://doi.org/10.1038/23196

Rubin, C. M. (1996). Systematic underestimation of earthquake magnitudes from large intracontinental reverse faults: Historical ruptures break across segment boundaries. *Geology*, *24*(11), 989. https://doi.org/10.1130/0091-7613(1996)024<0989:SUOEMF>2.3.CO;2

Rubin, C. M., Sieh, K., Chen, Y., Lee, J., Chu, H., Yeats, R., et al. (2001). Surface rupture and behavior of thrust faults probed in Taiwan. *Eos, Transactions American Geophysical Union*, *82*(47), 565–569. https://doi.org/10.1029/01EO00331

Scholz, C. H. (1982). Scaling laws for large earthquakes: Consequences for physical models. *Bulletin of the Seismological Society of America*, *72*(1), 1–14. https://doi.org/10.1785/BSSA0720010001

Stein, S., & Liu, M. (2009). Long aftershock sequences within continents and implications for earthquake hazard assessment. *Nature*, *462*(7269), 87–89. https://doi.org/10.1038/nature08502

Stockmeyer, J. M., Shaw, J. H., & Guan, S. (2014). Seismic hazards of multisegment thrust-fault ruptures: Insights from the 1906 Mw 7.4-8.2 Manas, China, earthquake. *Seismological Research Letters*, *85*(4), 801–808. https://doi.org/10.1785/0220140026

Toda, S., & Stein, R. S. (2018). Why aftershock duration matters for probabilistic seismic hazard assessment. *Bulletin of the Seismological Society of America*, *108*(3A), 1414–1426. https://doi.org/10.1785/0120170270

Wesnousky, S. G. (2006). Predicting the endpoints of earthquake ruptures. *Nature*, *444*(7117), 358–360. https://doi.org/10.1038/nature05275

Williams, J., Stirling, M., Langridge, R., Niroula, G., Vause, A., Stewart, J., et al. (2024). Along-strike extent of earthquakes on multi-segment reverse faults; insights from the Nevis-Cardrona fault, Aotearoa New Zealand. *Seismica*, *3*(2). https://doi.org/10.26443/seismica.v3i2.1310

Zhang, P.-Z., Wen, X., Shen, Z.-K., & Chen, J. (2010). Oblique, high-angle, listric-reverse faulting and associated development of strain: The Wenchuan earthquake of May 12, 2008, Sichuan, China. *Annual Review of Earth and Planetary Sciences*, *38*(1), 353–382. https://doi.org/10.1146/annurev-earth-040809-152602

References From the Supporting Information

Charreau, J., Chen, Y., Gilder, S., Dominguez, S., Avouac, J.-P., Sen, S., et al. (2005). Magnetostratigraphy and rock magnetism of the Neogene Kuitun He section (northwest China): Implications for late Cenozoic uplift of the Tianshan Mountains. *Earth and Planetary Science Letters*, *230*(1–2), 177–192. https://doi.org/10.1016/j.epsl.2004.11.002

Guan, S., Stockmeyer, J. M., Shaw, J. H., Plesch, A., & Zhang, J. (2016). Structural inversion, imbricate wedging, and out-of-sequence thrusting in the southern Junggar fold-and-thrust belt, northern Tian Shan, China. *AAPG Bulletin*, *100*(9), 1443–1468. https://doi.org/10.1306/04041615023

Wang, C. (2004). Crustal structure of the northern margin of the eastern Tien Shan, China, and its tectonic implications for the 1906 M∼7.7 Manas earthquake. *Earth and Planetary Science Letters*, *223*(1–2), 187–202. https://doi.org/10.1016/j.epsl.2004.04.015

Wang, W., Yin, H., Jia, D., Wu, Z., Wu, C., & Zhou, P. (2018). Calculating detachment depth and dip angle in sedimentary wedges using the area–depth graph. *Journal of Structural Geology*, *107*, 1–11. https://doi.org/10.1016/j.jsg.2017.11.014

Wu, X., Long, W., Li, Z., Wang, W., Yang, X., Sun, C., et al. (2024). Growth of the northeastern Tibetan Plateau since the middle Miocene as revealed by syn-tectonic growth strata. *Journal of Structural Geology*, *185*, 105176. https://doi.org/10.1016/j.jsg.2024.105176

Zhang, P., Deng, Q., Xu, X., Feng, X., Peng, S., Yang, X., et al. (1994). Blind thrust, fold earthquake, and the 1906 Manas earthquake in Xinjiang. *Seismology and Geology*, *16*(3), 193–204.